Complementarity of EIS and SPR to Reveal Specific and Nonspecific Binding When Interrogating a Model Bioaffinity Sensor; Perspective Offered by Plasmonic Based EIS

ARTICLE *in* ANALYTICAL CHEMISTRY · AUGUST 2014

Impact Factor: 5.64 · DOI: 10.1021/ac501348n · Source: PubMed

6 AUTHORS, INCLUDING:

Cristina Polonschii
International Centre of Biodynamics
18 PUBLICATIONS **71** CITATIONS
SEE PROFILE

Sorin David
International Centre of Biodynamics
18 PUBLICATIONS **76** CITATIONS
SEE PROFILE

Mihaela Gheorghiu
International Centre of Biodynamics
27 PUBLICATIONS **239** CITATIONS
SEE PROFILE

Eugen Gheorghiu
International Centre of Biodynamics
44 PUBLICATIONS **498** CITATIONS
SEE PROFILE

analytical chemistry

Article

pubs.acs.org/ac

Complementarity of EIS and SPR to Reveal Specific and Nonspecific Binding When Interrogating a Model Bioaffinity Sensor; Perspective Offered by Plasmonic Based EIS

Cristina Polonschii,[†] Sorin David,[†] Szilveszter Gáspár,[†] Mihaela Gheorghiu,[†] Mihnea Rosu-Hamzescu,[†,‡] and Eugen Gheorghiu*[,†,‡]

[†]International Centre of Biodynamics, 1B Intrarea Portocalelor, 060101 Bucharest, Romania

[‡]University of Bucharest, 4-12 Regina Elisabeta Blvd., 030018 Bucharest, Romania

Supporting Information

ABSTRACT: The present work compares the responses of a model bioaffinity sensor based on a dielectric functionalization layer, in terms of specific and nonspecific binding, when interrogated simultaneously by Surface Plasmon Resonance (SPR), non-Faradaic Electrochemical Impedance Spectroscopy (EIS), and Plasmonic based-EIS (P-EIS). While biorecognition events triggered a sensitive SPR signal, the related EIS response was rather negligible. Contrarily, even a limited nonspecific adsorption onto the surface of the metallic electrode, allowed by the intrinsic imperfect compactness of the functionalization layers, was signaled by EIS and not by SPR. The source of this finding has been addressed from both theoretical and experimental perspectives, demonstrating that EIS signals are mainly sensitive to adsorptions that alter the current pathway through defects of the functionalization layer exposing the electrode. These observations are of importance for those developing biosensors analyzed by SPR, EIS, or the novel combination of the two methods (P-EIS). A possible application of the observed complementarity of the two methods, namely assessment of sample purity in respect to a target analyte is highlighted. Moreover, the possibility of false-positive EIS responses (determined by nonspecific binding) when assessing samples containing complex matrices or consisting of small molecular weight analytes is emphasized.

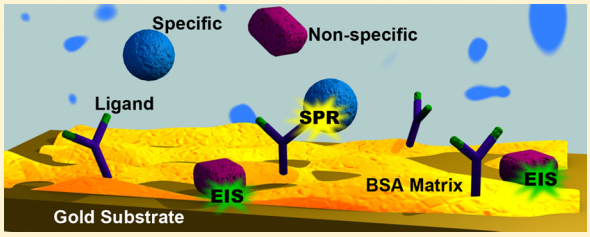

Surface Plasmon Resonance (SPR)[1−8] and Electrochemical Impedance Spectroscopy (EIS)[9−14] are among the few methods of choice used for label-free detection of bioaffinity complexes formed at the metal−liquid interface. SPR is a commercially mature method that displays excellent sensitivity in monitoring refractive index changes in the near vicinity of a sensing surface with plasmonic properties.[15] EIS is based on measuring the electrical current response to an AC potential applied between electrodes, being extremely sensitive to molecular adsorption taking place on the electrode surface.[13] EIS is used in conjunction with biosensors based on both conductive[16,17] and dielectric[12,18,19] functionalization layers to monitor affinity based interactions.

Faradaic EIS, involving redox probes, is often used to interrogate biosensors. Nevertheless, nonfaradaic EIS received increased interest as proved by several recently published papers which describe biosensors analyzed by nonfaradaic EIS.[20−24] This interest is motivated by the relative simplicity of nonfaradaic EIS as compared to faradaic EIS and by surface stability issues surrounding faradaic EIS—the cyanide ions from hexacyanoferrate compound were observed to etch functionalized gold with self-assembled monolayers (SAM).[25] This effect goes unnoticed and can be neglected when biosensors are built on massive gold electrodes and require short exposures to a hexacyanoferrate redox probe, but it grows into a significant problem when biosensors are built on thin gold films and require longer exposures. Thin film technology is widely employed for biosensor development as it is well suited for miniaturization and mass production. Biosensors interrogated without any redox probe by measuring the capacitive currents resulting from applying potential pulses rather than a sinusoidal potential[26−29] have been also reported. It is expected that the EIS related observations described by our study are valid and thus of interest for this class of capacitive biosensors as well.

Combined SPR-EIS approaches, involving thin gold layers (with thickness up to 50 nm), were also employed to observe bioaffinity interactions.[30−35] Moreover, recent studies demonstrated that it is possible to perform both SPR and electrical measurements based only on plasmonic detection[36−40] in the so-called plasmonic based electrochemical impedance spectroscopy (P-EIS). The technique has been innovatively used for both quantitative sensing and imaging. It was shown[37] that the SPR signal depends on surface charge density, which is modulated by applying an AC potential to the SPR sensor surface. Depending on experimental conditions, the AC component of the SPR response mainly reflects the capacitive

Received: October 30, 2013
Accepted: August 15, 2014
Published: August 15, 2014

   dx.doi.org/10.1021/ac501348n | *Anal. Chem.* 2014, 86, 8553−8562

component of the impedance.[38] Accordingly, the technique showed exquisite sensitivity for assessment of single cells and intracellular processes, catalytic nanoparticles, and biomolecular interactions.

To add specificity to these inherently nonspecific methods, the sensor/electrode surface is modified/functionalized with organic thin layers (e.g., SAMs, layers of conductive or nonconductive polymers, hydrogels, etc.) and subsequently with (bio)recognition elements selective to the target analyte. Among the different organic thin layers used to provide analytical specificity, SAMs made of alkanethiols are most popular. However, long-chain alkanethiols form defect-free monolayers, which act as thick barriers to electron transfer and ion penetration[41] and confer very high impedance. As a consequence, for sensors built with such SAMs, the EIS signal-to-noise ratio at low frequencies can be too low to be useful. On the other hand, short-chain alkanethiols assemble in thinner monolayers rendering high capacitance (therefore reduced capacitive reactance). However, these monolayers present pinhole defects allowing molecules to pass through and be nonspecifically adsorbed.[42] Moreover, for obtaining reproducible and selective biosensors, the deployed functionalization layers should exhibit negligible nonspecific binding. Reduction of nonspecific binding can be achieved by creating more hydrophilic interfaces, e.g. by including compounds such as polyethylene glycol derivatives in the surface functionalization steps[43] or by using a hydrophilic layer of cross-linked protein.[44]

Given the popularity of bioaffinity-based sensors, and of EIS, SPR, and P-EIS as methods of interrogation of such sensors, the purpose of this study is to identify both the similarities and the differences between the responses of the same antibody-modified interface interrogated with SPR and EIS (conventional EIS or P-EIS) in a flow injection setup.

As a model surface we used a hydrophilic layer of cross-linked protein (bovine serum albumin, BSA) previously demonstrated[44] to exhibit comparable characteristics with a commercially available, carboxymethylated dextran hydrogel (CM5 from GE Healthcare) in terms of specific and nonspecific binding. We bring evidence to the fact that the electrochemical signal has its source in unspecific binding events while the optical signal has its source in the bioaffinity complexes formed at the biosensor surface.

Although our study is not the first one involving combined EIS-SPR measurements, to the best of our knowledge, it is the first to address the source of the measured optical and electrical signals in terms of specific and nonspecific binding from a combined experimental and theoretical approach. As a direct consequence, the main constraints limiting the equivalence between conventional EIS and P-EIS responses are discussed.

EXPERIMENTAL SECTION

Materials. Bovine serum albumin (BSA), hexadecanoic acid (16-COOH), 11-mercapto 1-undecanol (11-OH), dithiodipropionic acid (2 × 3-COOH), human IgG (HIgG), affinity isolated antihuman IgG (AHIgG), antihuman IgG fraction of antiserum (serum AHIgG), biotin, *N*-hydroxysuccinimide (NHS), 1-ethyl-3-(dimethylaminopropyl) carbodiimide (EDC), and ethanolamine were purchased from Sigma–Aldrich (Germany). Fetal bovine serum (FBS) was purchased from Gibco. Succinic anhydride and sodium hypochlorite (NaOCl) were supplied by Acros Organics (Belgium). (1-Mercapto-11-undecyl)hexa(ethylene glycol)carboxylic acid (11-PEG-COOH) was purchased from Prochimia Surfaces, Poland. Surfactant P20 was provided by GE Healthcare. All of the other reagents for buffers were purchased from Sigma.

The buffers used for the experiments are phosphate buffer saline solution (PBS), pH 7.4, containing 137 mM NaCl, 10 mM phosphate, 2.7 mM KCl; immobilization buffer, 10 mM acetate buffer, pH 5; running buffer, HBS-EP buffer (10 mM HEPES, pH 7.4, 150 mM NaCl, 3 mM EDTA, 0.005% Surfactant P20).

Ultrapure water (Millipore) was used throughout the preparations. All chemical reagents were of analytical grade and were used without further purification.

Simultaneous SPR, EIS, and P-EIS Measurements—Basic Principle and Setup. A sinusoidal potential applied to the Au sensor (WE) determines both a current response (conventional EIS) and a SPR response (plasmonic-EIS). While the DC component of SPR response (obtained by averaging) provides the conventional SPR signal, its AC component is linked to EIS signal. It was previously[37,38] shown that the sinusoidal potential (ΔV) determines oscillations of the surface charge density (with amplitude $\Delta\sigma$) which induces oscillations of the SPR angle (with amplitude $\Delta\theta_{SPR}$). $\Delta\theta_{SPR}$ is proportional to $\Delta\sigma$ by a coefficient, α. Since $\Delta\sigma$ is also related to current density (ΔJ), α can be theoretically calculated or experimentally determined. Then admittance density is derived providing the impedance response based on the AC component of the SPR signal (see Supporting Information). Provided that impedance of the electrode interface is essentially due to the capacitive reactance, eq 9 from Supporting Information allows the assessment of both the amplitude and phase of the admittance density based on P-EIS signal, enabling comparison of P-EIS and conventional EIS. It also highlights the $\pi/2$ phase shift between $\Delta\theta_{SPR}$ and admittance (as measured by conventional EIS).

The setup (Figure 1) used in the study is based on a custom-made SPR system that has been developed[44] around the Spreeta TSPR1K23 SPR sensor (Texas Instruments, TX, USA). The system, assisted by a LabView dedicated program, allows acquisition of 230 SPR curves per second. The curves are fitted, and the SPR angle, i.e., the incidence angle corresponding to SPR minimum, is derived for each curve. The gold surface on

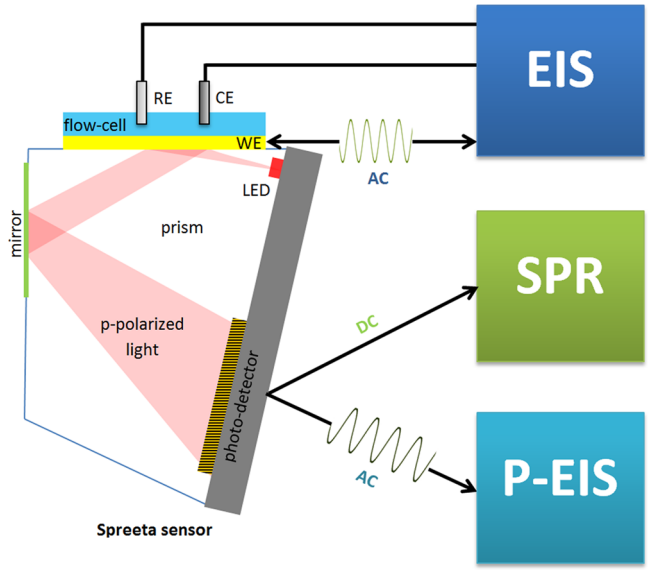

Figure 1. Schematic representation of the experimental setup.

dx.doi.org/10.1021/ac501348n | *Anal. Chem.* 2014, 86, 8553–8562

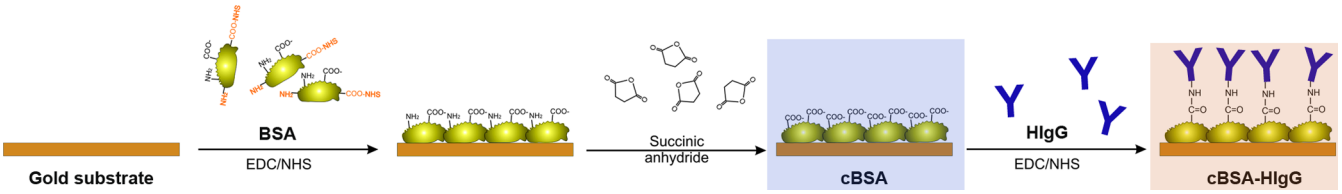

Figure 2. Schematic representation of the functionalization and immobilization steps.

the SPR sensor also serves as a working electrode for the conventional EIS and P-EIS measurements. A system consisting of an impedance analyzer (Solarton 1260 Impedance Analyzer) and a potentiostat (Solarton CellTest 1470E) applies a sinusoidal potential and a DC bias to the WE and provides the conventional EIS measurements. The SPR response to the potential modulation is analyzed, and $\Delta\theta_{SPR}$ is derived by Discrete Fourier Transform (DFT) while the SPR angle is obtained by averaging.

The electrochemical cell consisted of a three-electrode system: Ag/AgCl as reference electrode (RE), Pt as a counter electrode (CE), and the gold SPR surface as a working electrode. The system was measured by applying a signal of $0.2V_{pp}$, and 0.12 V bias vs RE (see Supporting Information), within a frequency range of 1−350 Hz. Running buffer was used as the electrolyte. The values for the AC amplitude and DC bias of the applied potential were chosen to augment the SPR response to AC signals, in line with previous studies[45,46] which showed that the SPR output is mainly influenced by positive potentials.

Contact Angle Measurements. A CAM 100 apparatus (KSV Instruments) consisting of a FireWire camera with 50 mm optics and a 40 mm extension tube, sample stage, syringe holder, and a LED based red background lightning was used to evaluate the hydrophilic properties. The contact angles are calculated by the CAM 100 Software by fitting the shape of the water drop with a Young−Laplace equation. The program calculates the contact angle for both sides of the droplet, and the result is represented as the mean value.

Experimental Constraints. Specific experimental conditions have to be considered when performing simultaneously EIS, SPR, and P-EIS measurements. EIS is sensitive to interface events only at rather low frequencies (at higher frequencies, the signal is modulated by the properties of the bulk solution). Moreover, depending on the electrical parameters of the sensing surface after functionalization, an optimal signal-to-noise ratio may require an increase of the lower limit of the measurement frequency domain. In addition, the limited SPR acquisition rate (∼200 spectra/s) restricts the experimental access to P-EIS up to a frequency of ∼50 Hz. Therefore, conventional EIS measurements were performed within the 1−350 Hz frequency range, whereas P-EIS was derived for the frequency providing an optimally high signal-to-noise ratio (3.5 Hz). For better comparison with P-EIS, the EIS signal is presented for the same single frequency (3.5 Hz), since similar behavior was registered for the whole 1−350 Hz frequency domain.

Choice of Functionalization Method. To compare responses of a biosensor in terms of specific and nonspecific binding when interrogated by SPR, EIS, and P-EIS, a suitable functionalization layer, which allows reproducible immobilization of the ligand (in our case HIgG), has a low nonspecific binding, and allows good signal-to-noise ratio EIS measurements, has to be implemented.

In preliminary tests, we used SAMs of alkanethiols, extensively exploited for both EIS[12,18,19] and SPR[47,48] measurements. Both short (2 × 3-COOH) and long chains alkanethiols (11-PEG-COOH and 1:25 mixture of 16-COOH and 11-OH) were investigated, in terms of nonspecific response (using EIS and SPR) and capability to render good signal-to-noise ratio EIS measurements. Surfaces functionalized with the short chain alkanethiol presented high nonspecific binding, when measured by both SPR and EIS. As expected, the ones functionalized with long chain thiols presented higher impedance (10−20 times higher than for short chain thiols) and better resistance to nonspecific binding, according to SPR measurements. Nevertheless, the poor signal-to-noise ratio achieved hinders the applicability of this functionalization method for both EIS and P-EIS measurements. Alternatively, a functionalization method based on carboxylated cross-linked BSA (cBSA) was investigated.

The method was selected because the cBSA functionalization layer consists of BSA molecules which are commonly used as a blocking agent to avoid nonspecific adsorption in bioaffinity assays[15] and because it has a hydrophilic character,[49] according to contact angle measurements in water (49.93 ± 0.23°, comparable with CM5, GE Healthcare −44.57 ± 0.16°, a commercially available sensor with a relatively low nonspecific binding[50]). Moreover, the carboxyl groups allow further immobilization of biomolecules via amino-coupling chemistry. The SPR sensor based on the cBSA platform was previously compared to the CM5 sensor, in terms of sensitivity, nonspecific binding, and stability.[44] cBSA exhibited a similar coefficient of variation (3.6% for CM5 and 5% for cBSA) in detecting thrombin in the presence of other interfering proteins (plasma) and proved stable during numerous injection−regeneration cycles.

Moreover, preliminary EIS measurements of cBSA functionalized sensors indicate impedance magnitudes (at low frequencies) similar to the ones obtained using short chain thiols and appropriate signal-to-noise ratios that warrant good biosensor sensitivity. Consequently, the functionalization layer was considered suitable for further testing of specific and nonspecific EIS and SPR responses.

Sensor Preparation. The sensor consisted of a 0.3 mm thick BK7 glass slide coated by thermal evaporation (Physical Vapor Deposition, Kurt J. Lesker, US) with 3 nm titanium followed by 47 nm gold. The Au sensor chip was sequentially cleaned with 5% NaOCl, deionized water, ethanol, and deionized water and finally dried under a nitrogen stream. The gold surface was afterward modified with thiols (48 h incubation in 1 mM solution in ethanol) or with cBSA, according to the protocol previously described.[44] Briefly, the first step involves the formation of a cross-linked BSA film by exposing the gold sensor to a mixture of BSA, EDC, and NHS solutions. Next, the sensor is incubated overnight, at room temperature, in succinic anhydride, to add carboxylic groups to the BSA film (Figure 2).

dx.doi.org/10.1021/ac501348n | Anal. Chem. 2014, 86, 8553−8562

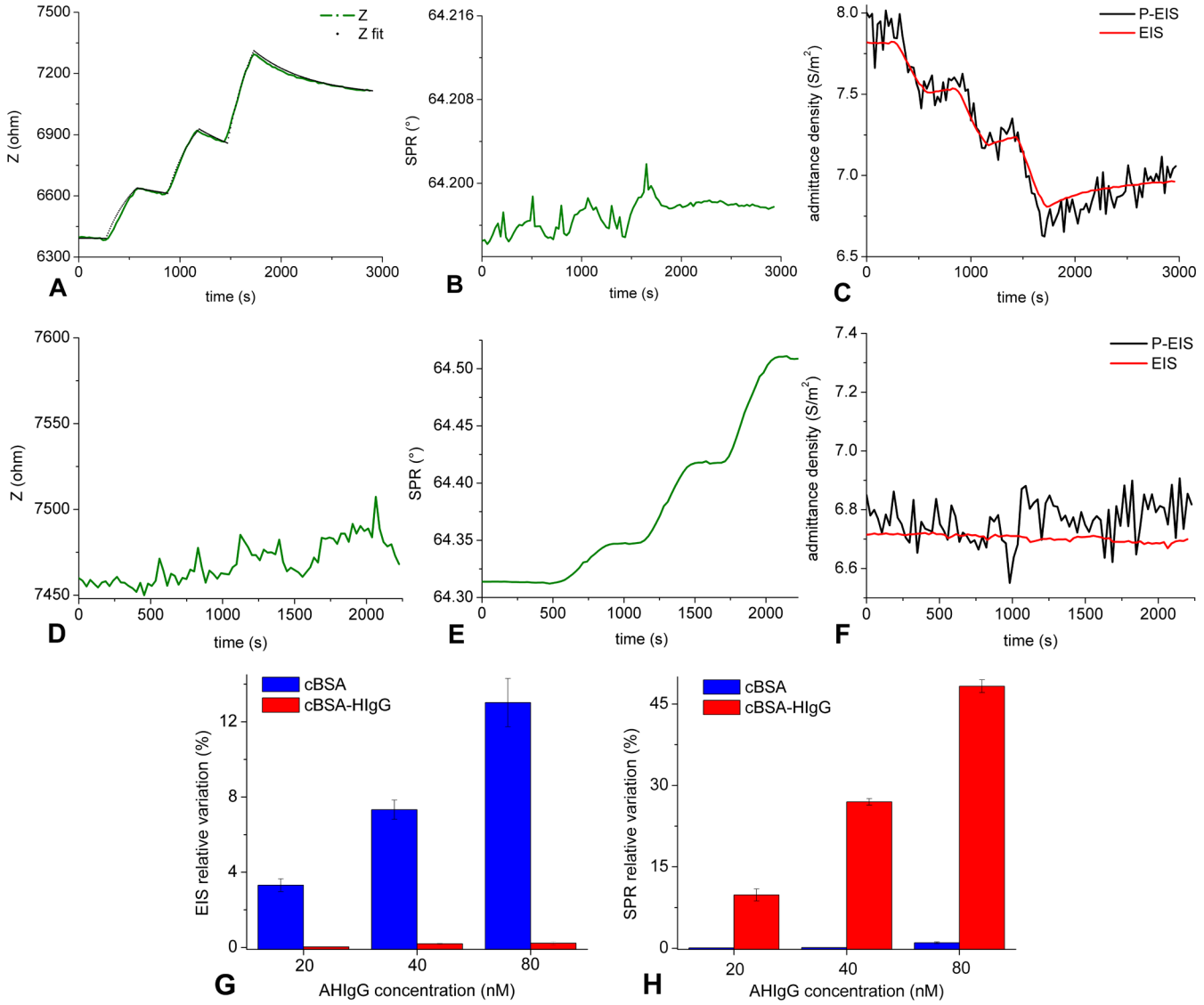

Figure 3. Responses to successive injections of increasing concentrations of pure AHIgG (20 nM, 40 nM, and 80 nM) on the cBSA surface (upper row) and cBSA-HIgG modified surface (lower row) revealed by EIS-impedance magnitude at 3.5 Hz (A, D), SPR (B, E), and admittance density at 3.5 Hz revealed by EIS and P-EIS (C, F). The dependence on AHIgG concentration of the relative variations of the EIS (G) and SPR (H) response.

For the HIgG immobilization procedure, the functionalized surface was activated for 7 min using 1:1 volumetric mixtures of 100 mM NHS and 400 mM EDC solutions, followed by a 20 min injection of 50 μg/mL HIgG in immobilization buffer and 7 min blocking with 1 M ethanolamine hydrochloride (pH 8.5). In the following, the immobilized sensor will be referred to as cBSA-HIgG.

Flow Cell. A polydimethylsiloxane (PDMS) gasket defined a flow channel on the WE. A polyether ether ketone (PEEK) lid, integrating the fluidic inlet and outlet, the RE, CE, and a spring loaded gold pin for electrical contact with WE (outside of the liquid channel), covered the PDMS gasket. The liquid sample was delivered through the flow cell by an automated fluidic system comprised of a syringe pump and valves actuated by dedicated software made in LabView.

Injection Protocol. The simultaneous SPR, EIS, and P-EIS measurements involved injections of different analyte molecules over cBSA or cBSA-HIgG modified surfaces. Electrical measurements showed, within preliminary tests, that following regeneration, the recovery of the initial state of the interface, can take a significantly longer time as compared to SPR signals. Therefore, aiming for a direct comparison of the three methods simultaneously used, while avoiding possible stability and binding capacity issues after regeneration steps, a successive injections protocol[51] was preferred against the one with regeneration steps between injections. All injections were performed at a 30 μL/min flow rate. For each injection, the sensor surface was exposed to the sample and then to the running buffer.

Nonspecific binding can be reduced by optimizing the composition of the running buffer. In general, physiological (150 mM) or higher salt concentrations reduce nonspecific electrostatic interactions.[52] Also, surfactants are widely employed in immunoassays to limit nonspecific adsorption of proteins due to hydrophobic interactions.[53] Therefore, both for injection and washing, a standard HBS buffer was used, comprising 163 mM salt and 0.005% surfactant P20, commonly reported in the literature as running buffer for bioaffinity interactions.

dx.doi.org/10.1021/ac501348n | Anal. Chem. 2014, 86, 8553−8562

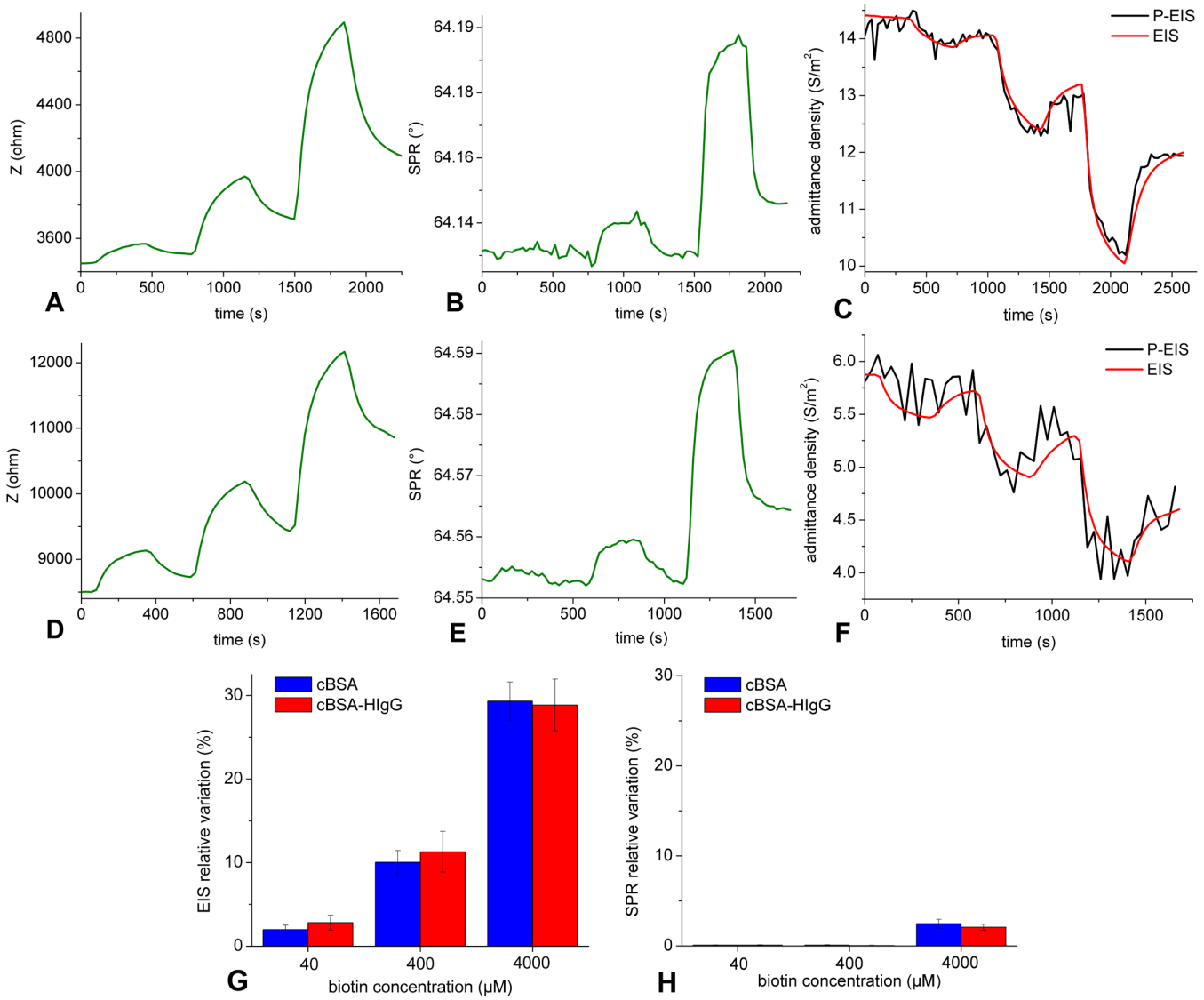

Figure 4. Responses to successive injections of increasing concentrations of biotin (40 μM, 400 μM, and 4 mM) on the cBSA surface (upper row) and cBSA-HIgG modified surface (lower row) revealed by EIS-impedance magnitude at 3.5 Hz (A, D), SPR (B, E) and admittance density at 3.5 Hz revealed by EIS and P-EIS (C, F). The dependence on biotin concentration of the relative variations of EIS (G) and SPR (H).

RESULTS AND DISCUSSION

To assess the SPR, EIS, and P-EIS responses in respect to specific and nonspecific binding, liquid samples containing the specific analyte, AHIgG, pure or mixed with serum or small molecular weight molecules were injected on (1) surfaces without ligands presenting affinity to the target analyte, i.e., functionalized merely with carboxylated BSA, cBSA, and (2) affinity sensors, i.e., cBSA sensors further immobilized with HIgG, cBSA-HIgG sensors. For each injection, the relative variation (R_v, %) of the signal was calculated based on the values recorded after the corresponding washing step (V_i) in respect to the initial baseline before injection (V_0), as follows: $R_v=((V_i - V_0)/V_0) \times 100$. V_i was chosen after a 4 min wash with running buffer. The chosen time interval was based on the flow cell volume and flow rate and represents the minimum time required to entirely replace the sample with running buffer.

SPR, EIS, and P-EIS Response of cBSA (Reference) and cBSA-HIgG (Specific) Sensors When Challenged with the Pure Target Analyte (AHIgG). Increasing concentrations (20 nM, 40 nM, and 80 nM) of affinity isolated AHIgG (~160 kDa MW) diluted in running buffer were injected over a cBSA surface.

Reflecting a low nonspecific adsorption of the cBSA surface, the SPR signal (Figure 3B) presented very small variations: 0.05 ± 0.01, 0.11 ± 0.005, and 1.01 ± 0.16% R_v. On the basis of the V_i value at the end of the successive injections, an estimated ~70 AHIgG molecules/μm^2 on the sensor surface can be inferred.[15]

In contrast, EIS and P-EIS signals (Figure 3A, C) varied consistently with antibody concentration: 3.3 ± 0.34, 7.33 ± 0.51, and 13.02 ± 1.28% R_v for 20, 40, and 80 nM, respectively, suggesting exquisite sensitivity to nonspecific adsorption.

When applying the same series of injections on the specific, cBSA-HIgG, surface, the SPR signal (Figure 3E) varied, as expected for a bioaffine modified surface, proportionally with antibody concentration: 9.82 ± 1.1, 26.96 ± 0.6, and 48.28 ± 1.18% R_v. A relative signal of 48.28% corresponds to a large number of AHIgG molecules affinity bound to HIgG (~4200 molecules/μm^2 at the end of the three successive injections).

dx.doi.org/10.1021/ac501348n | Anal. Chem. 2014, 86, 8553−8562

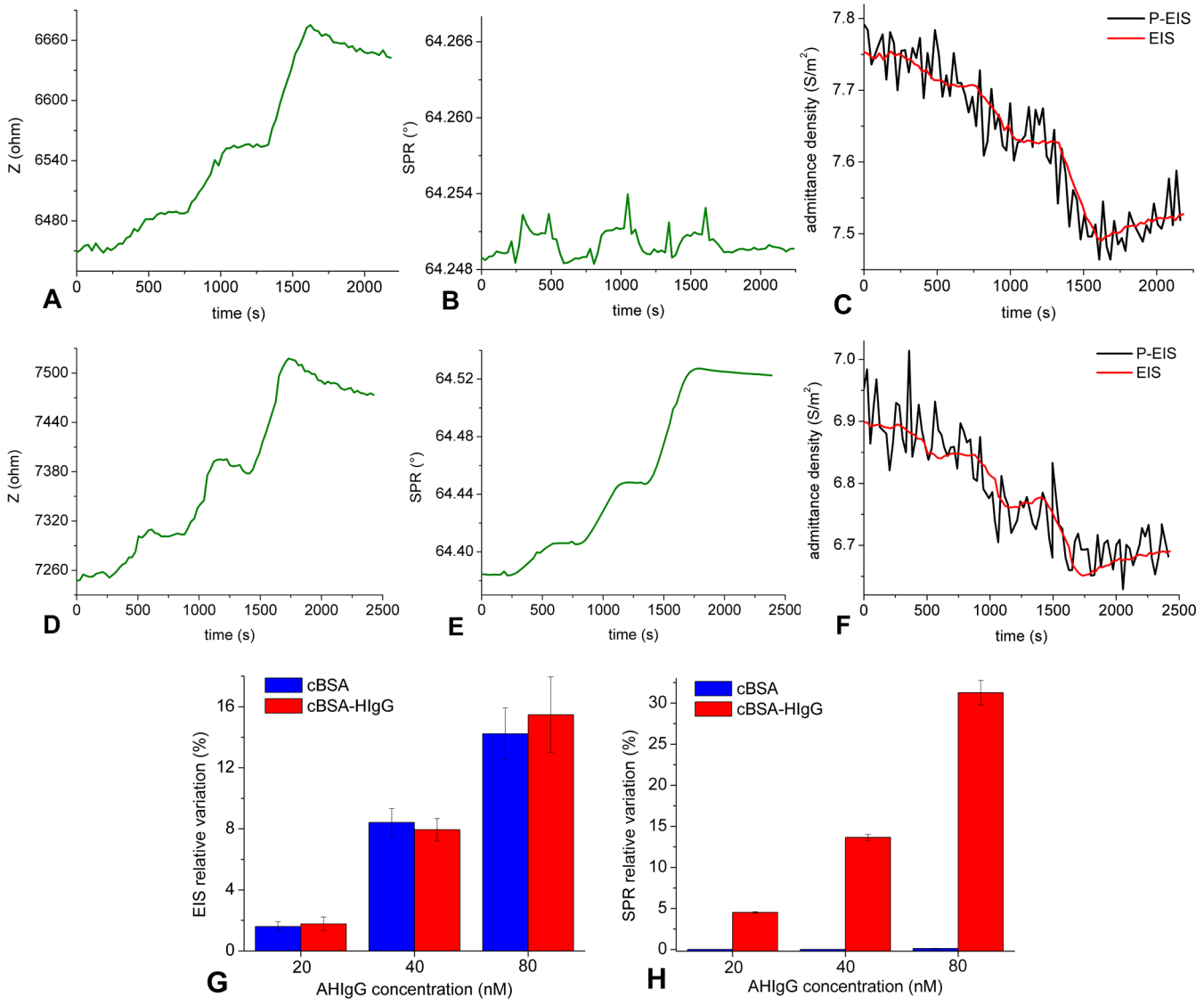

Figure 5. Responses to successive injections of increasing concentrations of serum AHIgG (20 nM, 40 nM, and 80 nM) on cBSA surface (upper row) and cBSA-HIgG modified surface (lower row) revealed by EIS-impedance magnitude at 3.5 Hz (A, C) and SPR (B, D). The dependence on serum AHIgG concentration of the relative variation of EIS (G) and SPR (H) signals.

Since the SPR signal was rather robust to nonspecific binding (i.e., when injecting AHIgG on cBSA surface), the SPR response registered after injecting AHIgG on the cBSA-HIgG surface is mostly determined by specific binding.

In contrast, EIS and P-EIS (Figures 3D,F) showed fairly negligible responses: 0.03 ± 0.0015, 0.195 ± 0.025, and 0.22 ± 0.082% R_v following the very same injections.

This contrast is even more pronounced when analyzing the relative variations of EIS (Figure 3G) and SPR (Figure 3H) for cBSA and cBSA-HIgG surfaces challenged with a high molecular weight compound (AHIgG). Although EIS was able to sense the effect of a small number of molecules that were nonspecifically bound, it was insensitive to a higher number (2 orders of magnitude) of AHIgG molecules specifically bound to the additional layer of immobilized HIgG.

These results indicate the EIS lack of sensitivity to binding events taking place farther from the electrode interface, as well as a strong response to nonspecific adsorption. One possible reason could be that the EIS signal is influenced by the compounds able to enter the nanoscopic defects (pinholes) of the functionalization layer and block the capacitive current. This has been further addressed by testing the effect of small molecules (biotin) able to reach the electrode surface.

SPR, EIS, and P-EIS Behavior of cBSA and cBSA-HIgG Sensors when Challenged with Solutions Comprising Various Concentrations of a Small Molecular Weight Compound. Next, we challenged cBSA and cBSA-HIgG sensors with biotin, a small molecular weight compound expected to easily pass through the defects of the functionalization layer. Increasing concentrations (40 μM, 400 μM, and 4 mM) of biotin (244.3 Da) diluted in running buffer were injected over cBSA and cBSA-HIgG surfaces.

Just as expected, the EIS and P-EIS signals varied with biotin concentration, for both surfaces. Electrical signals varied with more than 28% in the presence of 4 mM biotin (Figure 4A,C,D,F) proving the EIS sensitivity to small molecules able to penetrate nanoscopic defects and significantly modulate capacitive currents.

The SPR signals, sensitive to the mass of bound analyte, presented for both surfaces (Figures 4B,E) negligible 0.1%

dx.doi.org/10.1021/ac501348n | Anal. Chem. 2014, 86, 8553−8562

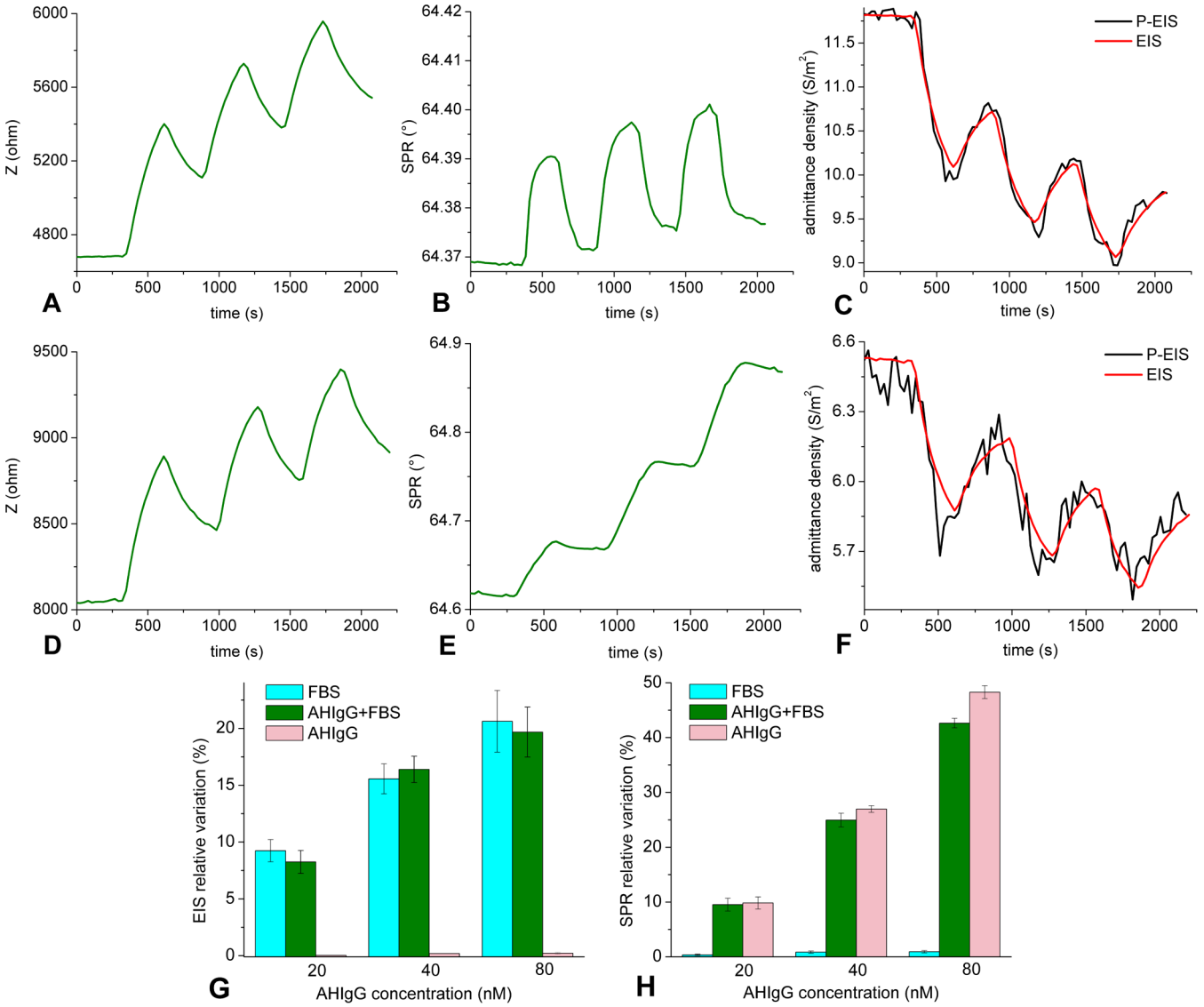

Figure 6. Responses to successive injections of diluted serum (FBS/HBS = 1:100, upper row) and increasing concentrations of AHIgG in diluted serum (lower row) on the cBSA-HIgG modified surface assessed by EIS-impedance magnitude at 3.5 Hz (A, D), SPR (B, E), and admittance density at 3.5 Hz revealed by EIS and P-EIS(C, F); comparison of the relative variation for cBSA-HIgG sensors measured by EIS (G) and SPR (H) when challenged in three sequential injections with FBS, increasing concentrations of AHIgG in diluted serum, and increasing concentrations of pure AHIgG (20, 40, and 80 nM).

variations for μM biotin concentrations and a mere 2% for the 4 mM concentration.

SPR, EIS, and P-EIS Behavior of cBSA and cBSA-HIgG Sensors when Challenged with the Analyte of Interest Mixed with Serum Components. As real samples are often characterized by complex matrices, and since not all commercially available antibodies are affinity purified, we set to investigate the nonspecific effect due to serum components as revealed by both SPR and EIS. Increasing concentrations (20, 40, and 80 nM) of serum AHIgG diluted in running buffer were injected over the cBSA surface.

EIS and P-EIS signals varied with serum AHIgG concentration: 1.59 ± 0.32, 8.42 ± 0.92, and 14.23 ± 1.68% R_v (Figure 5A,C), while the SPR signal presented, as expected, very small variations: 0.006 ± 0.002, 0.004 ± 0.001, and 0.10 ± 0.03% R_v (Figure 5B), corresponding to ∼20 AHIgG molecules/μm^2 adsorbed at the end of the injections.

When applying the same series of injections on the cBSA-HIgG surface, all EIS, P-EIS, and SPR signals varied with serum AHIgG concentration (Figures 5D,F,E). Accordingly, EIS response varied by 1.78 ± 0.45, 7.94 ± 0.73, and 15.47 ± 2.48% R_v and SPR response by 4.51 ± 0.11, 13.65 ± 0.36, and 31.26 ± 1.49% R_v, for 20, 40, and 80 nM serum AHIgG, corresponding to ∼3000 AHIgG molecules/μm^2 affinity bound at the end of the injections.

Injections of serum AHIgG on the cBSA surface render negligible nonspecific SPR signals; therefore, on the cBSA-HIgG surface the SPR responses are mostly determined by specific binding (Figure 5H). As previously shown, EIS was not sensitive to AHIgG binding to HIgG (Figure 3D) but sensed adsorption of small molecules also on the cBSA-HIgG surface (Figure 4D). Therefore, the EIS response obtained when injecting serum AHIgG on the cBSA-HIgG surface is due to nonspecific binding of small serum components (such as glucose, hormones, and vitamins[54]).

dx.doi.org/10.1021/ac501348n | Anal. Chem. 2014, 86, 8553−8562

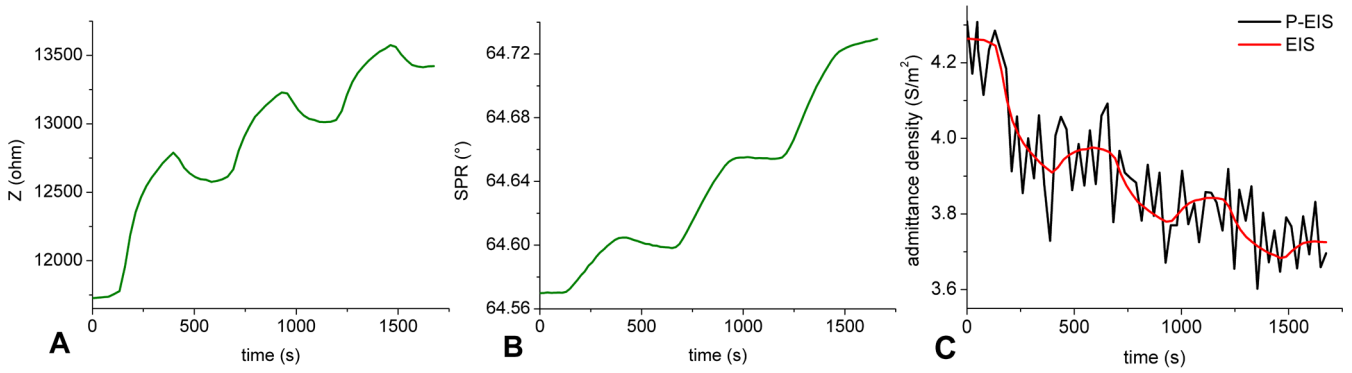

Figure 7. Responses to successive injections of AHIgG diluted in 400 μM biotin (20 nM, 40 nM, and 80 nM) on a cBSA-HIgG modified surface assessed by EIS-impedance magnitude at 3.5 Hz (A), SPR (B), and admittance density at 3.5 Hz revealed by EIS and P-EIS (C).

Table 1. Summary of the Studied Cases, Illustrating the Dependence of EIS and SPR Response on Sensor Surface and Sample Combinations[a]

	Maximum relative variation (%)				Figures (in order)
Method	EIS		SPR		
Surface / Analyte	cBSA	cBSA-HIgG	cBSA	cBSA-HIgG	
AHIgG	13.02±1.28	0.22±0.08	1.01±0.16	48.28±1.18	3A, 3D, 3B, 3E
biotin	29.32±2.27	28.85±3.08	2.47±0.49	2.09±0.34	4A, 4D, 4B, 4E
serum AHIgG	14.23±1.68	15.47±2.48	0.10±0.03	31.26±1.49	5A, 5D, 5B, 5E
FBS		20.61±2.72		0.93±0.21	6A, 6B
AHIgG+FBS		19.67±2.19		42.64±0.87	6D, 6E
AHIgG+biotin		14.38±1.56		34.85±1.81	7A, 7B

[a]Table cells colored in red mark the large responses, while the table cells colored in blue emphasize the small signals. A perfect match between expectations and measurements can be observed only for SPR.

To further investigate this finding, we used FBS as a model serum matrix and performed successive injections of the same concentration of FBS (1:100) diluted in HBS over cBSA-HIgG surface.

While EIS and P-EIS provide similar (nonspecific) signals which significantly varied with serum concentrations (Figures 6A,C), the SPR signal presented very small increments (Figure 6B). Accordingly, the EIS response varied by 9.24 ± 0.98, 15.55 ± 1.32, and 20.61 ± 2.72% R_v and SPR response by 0.36 ± 0.14, 0.85 ± 0.19, and 0.93 ± 0.21% R_v.

Then, we further added AHIgG to 1:100 diluted FBS in HBS and injected these solutions over a cBSA-HIgG modified sensor. Increasing concentrations (20, 40, and 80 nM) of AHIgG in diluted FBS determined the variation of EIS, P-EIS, and SPR signals (Figure 6D,F,E). Accordingly, EIS response varied by 8.25 ± 1.01, 16.38 ± 1.16, and 19.67 ± 2.19% R_v and SPR response by 9.52 ± 1.18, 24.95 ± 1.25, and 42.64 ± 0.87% R_v, corresponding to ~4000 AHIgG molecules/μm^2 affinity bound at the end of the injections.

These results fully support the assessment that when injecting either serum AHIgG or pure AHIgG in diluted FBS on cBSA-HIgG surfaces, the related EIS/P-EIS response is merely determined by the nonspecific binding of small serum components.

SPR, EIS, and P-EIS Behavior of cBSA and cBSA-HIgG Sensors When Challenged with Mixtures of the Analyte of Interest and a Small Molecule. To further substantiate the source of SPR and EIS/P-EIS responses, the following experiment was performed: mixtures of large and small molecules (AHIgG diluted in 400 μM biotin in HBS) were injected over cBSA-HIgG modified sensors. Increasing concentrations (20, 40, and 80 nM) of AHIgG diluted in 400 μM biotin determined significant variations of EIS, P-EIS, and SPR signals (Figure 7A,C,B).

Accordingly, EIS response varied by 7.29 ± 0.48, 10.96 ± 0.87, and 14.38 ± 1.56% R_v and SPR response by 7.74 ± 0.88, 19.11 ± 1.34, and 34.85 ± 1.81% R_v, corresponding to ~3700 AHIgG molecules/μm^2 affinity bound at the end of the injections.

Since the shift of the SPR angle reflects the amount of accumulated mass at the sensor surface,[15] the smaller the molecule adsorbed on the sensor surface, for the same concentration, the smaller the SPR signal. Therefore, small molecules, such as biotin, are practically invisible for SPR. Notably, as previously shown (Figure 4B,E), the SPR signal determined by 400 μM biotin was small and returned to the baseline before injection. Thus, in the case of mixture, the significant SPR signal, with a very small dissociation (Figure 7B) can be clearly attributed to specific AHIgG−HIgG binding. Conversely, the variation of the EIS signal in the case of the mixture is well correlated to the data on biotin injections (Figure 4G). As previously shown, EIS is not sensitive to AHIgG binding to HIgG (Figure 3D); therefore EIS signal is due to nonspecific binding of biotin.

Repeated injections of increasing concentrations of target analyte on cBSA surfaces (Figure 3B) and repeated injections of substances prone to nonspecific adsorption on cBSA-HIgG surfaces (Figure 6B) both resulted in negligible SPR responses (e.g., below ~2.2% maximum relative variation). In contrast, ~40% maximum relative variation of the SPR signal has been achieved for specific binding of the analyte whether alone or in complex matrices (Figures 3E and 6E). These results confirm

dx.doi.org/10.1021/ac501348n | Anal. Chem. 2014, 86, 8553−8562

the ability of SPR to discriminate between the analyte and interfering components, therefore evidencing the high selectivity of the sensor interrogated by SPR.

Table 1 below reunites the maximum responses revealed by EIS or SPR on nonimmobilized and specifically immobilized (i.e., cBSA and cBSA-HIgG) sensors when challenged with (1) the target analyte, (2) mixtures of target analyte and other constituents (susceptible for nonspecific binding), and (3) only substances prone to nonspecific adsorption.

Insights into EIS Sensitivity. Since we do not use a redox couple, for the potentials used within the study, the EIS signal is caused by non-Faradaic currents (associated with movement of electrolyte ions, reorientation of solvent dipoles, adsorption/desorption, etc. at the electrode−electrolyte interface). Imperfect adsorption of BSA to the gold surface and/or subsequent loss during sensor use can create pinholes where electrolyte and injected molecules have access to the gold surface. When injecting AHIgG onto cBSA modified sensors, a limited amount of these large macromolecules adsorbs due to the available defects. They make a large impact on the electrical signal but stay practically under the detection limit of SPR. Further immobilization of the cBSA surface with HIgG reduces even more the number (and/or the size) of defects in the insulating BSA layer. Moreover, it produces plenty of sites for affinity binding. This assumption was also confirmed by injecting small molecules (e.g., biotin) that can fit better into the pinholes of the BSA layer and consequently have good blocking abilities. The large EIS signals induced by these small molecules on both sensors (cBSA and cBSA-HIgG) suggest that indeed the compounds were able to enter the pinholes and block the capacitive current (Figure 4G).

Therefore, the EIS signal must come from the injected molecules that adsorb at the metallic interface. A theoretical approach describing this finding (see Figure 3A) is presented in the Supporting Information. Upon repeated injections, the evolution of the impedance modulus at a specific frequency (i.e., 3.5 Hz) resembled the one achieved experimentally.

Even though the BSA film has similar impedance with the short chain thiol (∼ kohms at low frequencies), it is more robust to nonspecific binding (as revealed by SPR and EIS). A possible explanation is that the BSA film is a multilayered structure, with intricate three-dimensional defects easily accessed by small molecules, but posing a challenge to big molecules, whereas the thiol is a planar structure and defects may be accessible to either small or big molecules. Also, the hydrophilic properties of BSA further reduce nonspecific binding. These findings are not entirely new: a previous study[33] also acknowledged that adsorption of proteins on alkanethiol layers was accompanied by both SPR and impedance changes and that, on the contrary, the binding of the same proteins to gangliosides inserted in a lipid layer assembled over a thiol layer determined no changes in impedance (between 6 and 19996 Hz), but a significant SPR response.

Analytical Relevance. These experiments emphasize that, when analyzing samples comprising mixtures of the target analyte and low molecular weight compounds or complex media of different dilutions, both SPR and EIS methods are susceptible to providing significant concentration dependent results; however, these signals have complementary origins. Whereas SPR indicates the specific binding, the EIS/P-EIS provides information on the nonspecific adsorption. As such, our results open up a whole new application realm for the combination of EIS and SPR, which seems especially suitable to evaluate sample purity and the quality of the functionalization layer.

An application of the combined SPR-EIS analysis could be the assessment of both sample purity (e.g., residual biotin when using biotinylation kits) and concentration. Biotinylation (labeling molecules, e.g., proteins, oligonucleotides, etc. with biotin) is widely used to enable isolation, separation, concentration, and further downstream processing and analysis of biomolecules. Free biotin in the sample reduces the binding capacity by occupying the binding sites on the streptavidin and hence it should be effectively removed. To demonstrate the merit of SPR-EIS combination, real samples containing biotinylated HIgG molecules collected after a couple of purification steps were analyzed (results are presented in the Supporting Information). By using a single analytical method (the combined EIS-SPR approach) it was possible to evaluate if (1) the HIgG is effectively biotinylated (SPR response) and (2) the purification method is efficient (EIS/P-EIS response).

■ CONCLUSIONS

This study demonstrates the complementarity of SPR and EIS (conventional EIS or P-EIS) to appraise both specific and nonspecific binding when simultaneously analyzing the same bioaffinity sensor based on a dielectric functionalization layer.

While affinity binding events trigger a sensitive SPR signal, the EIS response is rather negligible. Contrarily, even a limited nonspecific adsorption is signaled by EIS, showing a previously unreported sensitivity to nonspecific binding, overarching the one to specific interaction, whereas related SPR response is insignificant.

Experimental and theoretical analysis based on a kinetic model and an equivalent circuit (Figure S-2, Supporting Information) link the observed high sensitivity of EIS to events impeding the capacitive current flow (e.g., substances blocking the pinholes or being directly adsorbed to the gold interface through the pinholes) hence to nonspecific binding.

As experimentally demonstrated, the P-EIS signal is consistent with the conventional EIS. We also theoretically relate the P-EIS signal to the conventional EIS and highlight the related constraints; i.e., impedance of the interface mainly exhibits a capacitive behavior, as the case of cBSA and cBSA-HIgG sensors.

Our results open up a whole new application realm for the combination of EIS and SPR, which seems especially suitable to evaluate sample purity and the quality of the functionalization layer. As an advantageous alternative, P-EIS can provide both SPR and EIS response, while using a simplified setup (AC current measurements are no longer required, as in standard Gain-Phase EIS Analyzers). While SPR angle derived from the DC component of the P-EIS signal reveals the concentration of the analyte of interest, the impedance response based on the AC component reports on contaminants and/or the defects within the functionalization layer.

For sensors based on dielectric functionalization layers, this study highlights the significant likelihood of false-positive EIS responses (determined by nonspecific binding) when assessing samples: (1) containing complex matrices (e.g., coping with dilutions of both serum and target analyte) or (2) consisting of small molecular weight analytes.

dx.doi.org/10.1021/ac501348n | Anal. Chem. 2014, 86, 8553−8562

■ ASSOCIATED CONTENT

Supporting Information

Equivalent circuit and a kinetic model of non-specific interaction monitored by EIS, bias effect on impedance measurements and SPR AC response, relating plasmonic-EIS signal to the impedance measured by conventional EIS, and experiments on real samples. This material is available free of charge via the Internet at http://pubs.acs.org.

■ AUTHOR INFORMATION

Corresponding Author

*E-mail: egheorghiu@biodyn.ro.

Notes

The authors declare no competing financial interest.

■ ACKNOWLEDGMENTS

The study was supported by the Romanian National Contract No. 11/2012, ID: PN II-ID-PCCE-2011-2-0075, BIOSCOPE project and by Romanian-Swiss Research Program Contract No. 7/2013, TumorAnalyzer.

■ REFERENCES

(1) Homola, J. *Chem. Rev.* **2008**, *108*, 462−493.
(2) Treviño, J.; Calle, A.; Rodríguez-Frade, J. M.; Mellado, M.; Lechuga, L. M. *Talanta* **2009**, *78*, 1011−1016.
(3) Wang, J.; Lv, R.; Xu, J.; Xu, D.; Chen, H. *Anal. Bioanal. Chem.* **2008**, *390*, 1059−1065.
(4) Tombelli, S.; Minunni, M.; Luzi, E.; Mascini, M. *Bioelectrochemistry* **2005**, *67*, 135−141.
(5) Manera, M.; Spadavecchia, J.; Leone, a; Quaranta, F.; Rella, R.; Dellatti, D.; Minunni, M.; Mascini, M.; Siciliano, P. *Sens. Actuators, B* **2008**, *130*, 82−87.
(6) Meyer, M. H. F.; Hartmann, M.; Keusgen, M. *Biosens. Bioelectron.* **2006**, *21*, 1987−1990.
(7) Dutra, R. F.; Kubota, L. T. *Clin. Chim. Acta* **2007**, *376*, 114−120.
(8) Hong, S. C.; Chen, H.; Lee, J.; Park, H.-K.; Kim, Y. S.; Shin, H.-C.; Kim, C.-M.; Park, T. J.; Lee, S. J.; Koh, K.; Kim, H.-J.; Chang, C. L.; Lee, J. *Sens. Actuators, B* **2011**, *156*, 271−275.
(9) Li, A.; Yang, F.; Ma, Y.; Yang, X. *Biosens. Bioelectron.* **2007**, *22*, 1716−1722.
(10) Zhang, Z.; Yang, W.; Wang, J.; Yang, C.; Yang, F.; Yang, X. *Talanta* **2009**, *78*, 1240−1245.
(11) Daniels, J. S.; Pourmand, N. *Electroanalysis* **2007**, *19*, 1239−1257.
(12) Xiao, F.; Zhang, N.; Gu, H.; Qian, M.; Bai, J.; Zhang, W.; Jin, L. *Talanta* **2011**, *84*, 204−211.
(13) Katz, E.; Willner, I. *Electroanalysis* **2003**, *15*, 913−947.
(14) Pui, T. S.; Kongsuphol, P.; Arya, S. K.; Bansal, T. *Sens. Actuators, B* **2013**, *181*, 494−500.
(15) Schasfoort, R. B. M.; Tudos, A. J. *Handbook of Surface Plasmon Resonance*; Schasfoort, R. B. M., Tudos, A. J., Eds.; Royal Society of Chemistry: Cambridge, 2008; pp 184−195.
(16) Sadik, O. A.; Xu, H.; Gheorghiu, E.; Andreescu, D.; Balut, C.; Gheorghiu, M.; Bratu, D. *Anal. Chem.* **2002**, *74*, 3142−3150.
(17) Chen, C.-S.; Chang, K.-N.; Chen, Y.-H.; Lee, C.-K.; Lee, B. Y.-J.; Lee, A. S.-Y. *Biosens. Bioelectron.* **2011**, *26*, 3072−3076.
(18) Zór, K.; Ortiz, R.; Saatci, E.; Bardsley, R.; Parr, T.; Csöregi, E.; Nistor, M. *Bioelectrochemistry* **2009**, *76*, 93−99.
(19) Wu, C.-C.; Lin, C.-H.; Wang, W.-S. *Talanta* **2009**, *79*, 62−67.
(20) Luo, X.; Xu, M.; Freeman, C.; James, T.; Davis, J. J. *Anal. Chem.* **2013**, *85*, 4129−4134.
(21) Ebrahimi, A.; Dak, P.; Salm, E.; Dash, S.; Garimella, S. V.; Bashir, R.; Alam, M. A. *Lab Chip* **2013**, *13*, 4248−4256.
(22) Caballero, D.; Martinez, E.; Bausells, J.; Errachid, A.; Samitier, J. *Anal. Chim. Acta* **2012**, *720*, 43−48.
(23) Tran, D. T.; Vermeeren, V.; Grieten, L.; Wenmackers, S.; Wagner, P.; Pollet, J.; Janssen, K. P. F.; Michiels, L.; Lammertyn, J. *Biosens. Bioelectron.* **2011**, *26*, 2987−2993.
(24) Qureshi, A.; Gurbuz, Y.; Kallempudi, S.; Niazi, J. H. *Phys. Chem. Chem. Phys.* **2010**, *12*, 9176−9182.
(25) Dijksma, M.; Boukamp, B. A.; Kamp, B.; van Bennekom, W. P. *Langmuir* **2002**, *18*, 3105−3112.
(26) Thipmanee, O.; Samanman, S.; Sankoh, S.; Numnuam, A.; Limbut, W.; Kanatharana, P.; Vilaivan, T.; Thavarungkul, P. *Biosens. Bioelectron.* **2012**, *38*, 430−435.
(27) Teeparuksapun, K.; Hedström, M.; Wong, E. Y.; Tang, S.; Hewlett, I. K.; Mattiasson, B. *Anal. Chem.* **2010**, *82*, 8406−8411.
(28) Wongkittisuksa, B.; Limsakul, C.; Kanatharana, P.; Limbut, W.; Asawatreratanakul, P.; Dawan, S.; Loyprasert, S.; Thavarungkul, P. *Biosens. Bioelectron.* **2011**, *26*, 2466−2472.
(29) Labib, M.; Hedström, M.; Amin, M.; Mattiasson, B. *Anal. Chim. Acta* **2010**, *659*, 194−200.
(30) Bart, M.; Os, P. J. H. J.; Van Kamp, B.; Bult, A.; Van Bennekom, W. P. *Sens. Actuators* **2002**, *84*, 129−135.
(31) Souto, D. E. P.; Silva, J. V.; Martins, H. R.; Reis, A. B.; Luz, R. C. S.; Kubota, L. T.; Damos, F. S. *Biosens. Bioelectron.* **2013**, *46*, 22−29.
(32) Sriwichai, S.; Baba, A.; Phanichphant, S.; Shinbo, K.; Kato, K.; Kaneko, F. *Sens. Actuators, B* **2010**, *147*, 322−329.
(33) Terrettaz, S.; Stora, T.; Duschl, C.; Vogel, H. *Langmuir* **1993**, *9*, 1361−1369.
(34) Helali, S.; Fredj, H.; Cherif, K.; Abdelghani, a; Martelet, C.; Jaffrezicrenault, N. *Mater. Sci. Eng., C* **2008**, *28*, 588−593.
(35) Lê, H. Q. a; Sauriat-Dorizon, H.; Korri-Youssoufi, H. *Anal. Chim. Acta* **2010**, *674*, 1−8.
(36) Shan, X.; Patel, U.; Wang, S.; Iglesias, R.; Tao, N. *Science* **2010**, *327*, 1363−1366.
(37) Foley, K. J.; Shan, X.; Tao, N. J. *Anal. Chem.* **2008**, *80*, 5146−5151.
(38) Lu, J.; Wang, W.; Wang, S.; Shan, X.; Li, J.; Tao, N. *Anal. Chem.* **2012**, *84*, 327−333.
(39) MacGriff, C.; Wang, S.; Wiktor, P.; Wang, W.; Shan, X.; Tao, N. *Anal. Chem.* **2013**, *85*, 6682−6687.
(40) Wang, W.; Foley, K.; Shan, X.; Wang, S.; Eaton, S.; Nagaraj, V. J.; Wiktor, P.; Patel, U.; Tao, N. *Nat. Chem.* **2011**, *3*, 249−255.
(41) Gooding, J. J.; Mearns, F.; Yang, W.; Liu, J. *Electroanalysis* **2003**, *15*, 81−96.
(42) Campuzano, S.; Pedrero, M.; Montemayor, C.; Fatás, E.; Pingarrón, J. M. *J. Electroanal. Chem.* **2006**, *586*, 112−121.
(43) Wijaya, E.; Lenaerts, C.; Maricot, S.; Hastanin, J.; Habraken, S.; Vilcot, J.-P.; Boukherroub, R.; Szunerits, S. *Curr. Opin. Solid State Mater. Sci.* **2011**, *15*, 208−224.
(44) Polonschii, C.; David, S.; Tombelli, S.; Mascini, M.; Gheorghiu, M. *Talanta* **2010**, *80*, 2157−2164.
(45) McIntyre, J. D. E. *Surf. Sci.* **1973**, *37*, 658−682.
(46) Kötz, R.; Kolb, D. M.; Sass, J. K. *Surf. Sci.* **1977**, *69*, 359−364.
(47) Taylor, a; Ladd, J.; Etheridge, S.; Deeds, J.; Hall, S.; Jiang, S. *Sens. Actuators, B* **2008**, *130*, 120−128.
(48) Tsai, W.-C.; Li, I.-C. *Sens. Actuators, B* **2009**, *136*, 8−12.
(49) Ostuni, E.; Chapman, R. G.; Holmlin, R. E.; Takayama, S.; Whitesides, G. M. *Langmuir* **2001**, *17*, 5605−5620.
(50) Lofas, S.; Johnsson, B. *J. Chem. Soc., Chem. Commun.* **1990**, 1526−1528.
(51) Karlsson, R.; Katsamba, P. S.; Nordin, H.; Pol, E.; Myszka, D. G. *Anal. Biochem.* **2006**, *349*, 136−147.
(52) *Biacore Sensor Surface Handbook*; Biacore: Sweden, 2003; pp 84−85.
(53) Brogan, K. L.; Shin, J. H.; Schoenfisch, M. H. *Langmuir* **2004**, *20*, 9729−9735.
(54) Lindl, T. *Zell- und Gewebekultur*, 5th ed.; Spektrum Akademischer Verlag: Heidelberg, Germany, 2002.